Available online at www.sciencedirect.com
SCIENCE DIRECT®
Archives of Biochemistry and Biophysics 422 (2004) 91–102
ABB
www.elsevier.com/locate/yabbi

Anthocyanidin reductases from *Medicago truncatula* and *Arabidopsis thaliana*

De-Yu Xie, Shashi B. Sharma, and Richard A. Dixon*

Plant Biology Division, Samuel Roberts Noble Foundation, 2510 Sam Noble Parkway, Ardmore, OK 73401, USA

Received 19 November 2003, and in revised form 5 December 2003

Abstract

Anthocyanidin reductase (ANR), encoded by the *BANYULS* gene, is a newly discovered enzyme of the flavonoid pathway involved in the biosynthesis of condensed tannins. ANR functions immediately downstream of anthocyanidin synthase to convert anthocyanidins into the corresponding 2,3-*cis*-flavan-3-ols. We report the biochemical properties of ANRs from the model legume *Medicago truncatula* (MtANR) and the model crucifer *Arabidopsis thaliana* (AtANR). Both enzymes have high temperature optima. MtANR uses both NADPH and NADH as reductant with slight preference for NADPH over NADH. In contrast, AtANR only uses NADPH and exhibits positive cooperativity for the co-substrate. MtANR shows preference for potential anthocyanidin substrates in the order cyanidin > pelargonidin > delphinidin, with typical Michaelis–Menten kinetics for each substrate. In contrast, AtANR exhibits the reverse preference, with substrate inhibition at high concentrations of cyanidin and pelargonidin. (+)-Catechin and (±)-dihydroquercetin inhibit AtANR but not MtANR, whereas quercetin inhibits both enzymes. Possible catalytic reaction sequences for ANRs are discussed.

Keywords: Condensed tannins; Flavonoids; Anthocyanidin; Kinetics; Model legume

Condensed tannins (CTs)[1] are oligomers or polymers of flavonoid units (flavan-3-ols, also known as catechins) linked by single C_4–C_8 or C_4–C_6 carbon–carbon bonds (Fig. 1A). CTs occur widely throughout the plant kingdom, often in seed coats but also in other tissues such as leaves, flowers, and stems. They play protective functions in the plant, particularly against herbivores [1,2], and have recently attracted considerable attention in view of their potentially beneficial effects on human and animal health [1–3]. CTs bind reversibly to proteins, and the tannins present in the leaves of some forage legumes such as *Desmodium uncinatum* and *Lotus corniculatus* can thereby slow the rate of protein degradation in the rumen and thus protect cattle and sheep from pasture bloat [1,3]. CTs are also powerful antioxidants, and this property may explain their beneficial effects on cardiac health and immunity [4,5]. The flavan-3-ol building blocks of CTs are also antioxidants [6,7], and clinical studies have shown protective effects of catechin, epicatechin, gallocatechin, and epigallocatechin against stomach cancer [8]. It has recently been shown that epicatechin present in dark chocolate has potential to promote cardiovascular health in humans [9].

CTs share the same upstream biosynthetic pathway as the anthocyanin flower pigments (Fig. 1A), and this pathway has been well defined at both the biochemical and molecular genetic levels [10,11]. It was previously believed that the branch point between the CT and anthocyanin pathways occurred at the level of leucoanthocyanidin, which is converted to anthocyanidin by the action of leucoanthocyanidin dioxygenase (also known as anthocyanidin synthase, ANS) and, hypothetically, to flavan-3-ol by a leucoanthocyanidin reductase (LAR). However, this model, which did not explain the origin of the 2,3-*cis* stereochemistry predominant in the building blocks of many CTs, has recently undergone revision as

* Corresponding author. Fax: 1-580-224-6692.
E-mail address: radixon@noble.org (R.A. Dixon).

[1] *Abbreviations used:* CT, condensed tannin; Mt, *Medicago truncatula*; At, *Arabidopsis thaliana*; ANR, anthocyanidin reductase; ANS, anthocyanidin synthase; LAR, leucoanthocyanidin reductase; DHQ, dihydroquercetin; MBP, maltose-binding protein; MDAR, monodehydroascorbate reductase; DFR, dihydroflavonol reductase.

0003-9861/$ - see front matter © 2003 Elsevier Inc. All rights reserved.
doi:10.1016/j.abb.2003.12.011

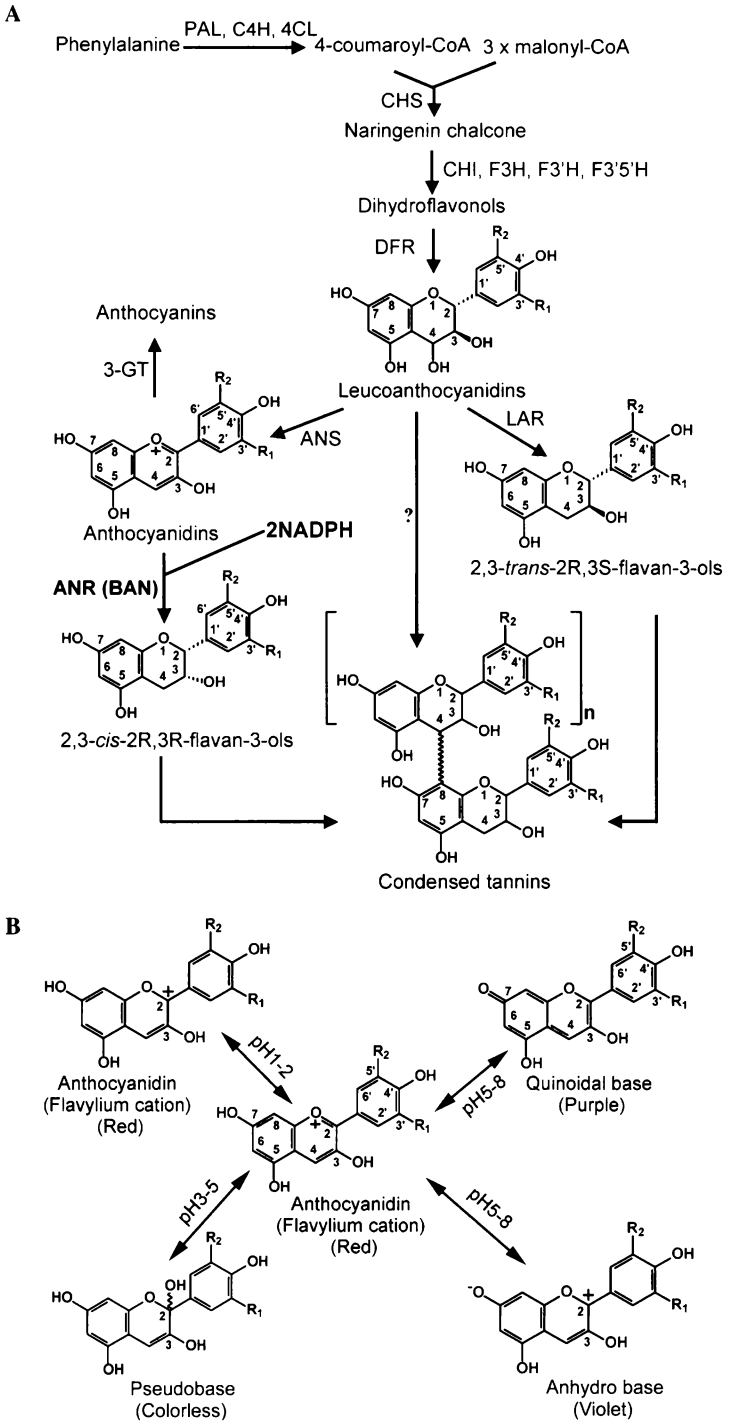

Fig. 1. (A) Schematic representation of the condensed tannin and anthocyanin biosynthetic pathways. PAL, L-phenylalanine ammonia-lyase; C4H, cinnamate-4-hydroxylase; 4CL, 4-coumarate: CoA-ligase; CHI, chalcone isomerase; CHS, chalcone synthase; F3H, flavanone 3-hydroxylase; F3′H, flavonoid 3′-hydroxylase; F3′5′H, flavonoid 3′,5′-hydroxylase; DFR, dihydroflavonol 4-reductase; LAR, leucoanthocyanidin reductase; ANS, anthocyanidin synthase (LDOX, leucoanthocyanidin dioxygenase); 3-GT, 3-glucosyl transferase; and ANR (BAN), anthocyanidin reductase (BANYULS). (B) Schematic representation of pH-dependent structural transformations of anthocyanidin in aqueous solution. R_1, R_2 = H or OH.

a result of the biochemical characterization of the *BANYULS* gene [12].

The *BANYULS* gene was named after the color of a French red wine for a mutant of *Arabidopsis thaliana* that lacked CTs in the seed coat endothelium and precociously accumulated anthocyanins [13,14]. It was originally proposed that *BANYULS* might encode LAR [14]. However, when expressed in *Escherichia coli*, the product of a *BANYULS* ortholog from the model legume *Medicago truncatula* efficiently converted antho-

cyanidins into their corresponding flavan-3-ols in the presence of NADPH [12]. This resulted in the proposal of a new pathway to CTs in which anthocyanidins were key intermediates, as substrates for the *BANYULS* gene product anthocyanidin reductase (ANR). Chemical characterization of the reaction products of ANR identified two isomers of flavan-3-ol, namely 2R, 3R-2, 3-*cis*-and 2S, 3R-2, 3-*trans* [12]. With cyanidin as substrate, these products are (−)-epicatechin and (−)-catechin, respectively. The 2R, 3R-2, 3-*cis*-flavan-3-ol, which was the major reaction product, is the common building block of CTs in many plants including *Arabidopsis* [15] and alfalfa (*Medicago sativa*) [16].

Recently, a *LAR* gene has been cloned following purification of the corresponding enzyme from *D. uncinatum* leaf tissue and shown to be a member of the isoflavone reductase (IFR)-like gene family. The enzyme converted radiolabeled leucocyanidin to (+)-catechin (2R, 3S-2, 3-*trans*-flavan-3-ol) [17]. (+)-Catechin is often the starter unit for CT polymerization. Together, ANR and LAR would therefore appear to be sufficient for formation of most monomeric building blocks of CTs. However, still very little is understood concerning the biological processes resulting in CT polymerization, or the reaction mechanisms whereby the building blocks are produced via ANR and LAR.

The basic anthocyanidin structure is generally considered to be the colored flavylium cation or salts thereof (Fig. 1B) [18–22]. However, anthocyanidins are not stable in aqueous solution and undergo rapid, pH-dependent, reversible transformations (Fig. 1B) [18,22,23]. The colors fade rapidly in weakly acidic solutions (pH 3–5), presumably due to formation of an equilibrium mixture of the flavylium cation and the colorless chromen-2-ol pseudobase (Fig. 1B) [22]. At pH 5–8, anthocyanidins can also rapidly transform to the anhydro base or quinoidal base (Fig. 1B) [22,23]. These transformations complicate the assignment of a reaction mechanism to ANR.

We here present a comparative study of the biochemical properties of ANRs from *M. truncatula* and *A. thaliana*. A full understanding of the mode of catalysis by ANR will facilitate future attempts to engineer condensed tannins or catechins in a variety of plant species for improving nutritional and health-related traits. Interestingly, the ANR enzymes from these two sources have quite different substrate specificities and kinetic properties. We present hypothetical mechanisms for the ANR reaction.

Materials and methods

Chemicals

Cyanidin chloride, pelargonidin chloride, and delphinidin chloride were purchased from Indofine (Hillsborough, NJ, USA). Ten mM methanol stock solutions were stored at −20 °C. NADPH and NADH were from Sigma (St. Louis, MO) and solutions were freshly prepared in cold reaction buffer when used for enzymatic assay. (+)-Catechin, (±)-catechin, (−)-epicatechin, (−)-gallocatechin, (−)-epigallocatechin, (±)-dihydroquercetin (DHQ), and quercetin were from Sigma, and methanolic stock solutions were stored at −20 °C.

Expression of MtANR and AtANR in E. coli

The open reading frame of the *MtANR* gene was amplified by polymerase chain reaction (PCR) using pSE380-BAN plasmid as template [12]. The amino terminal primer, 5′-GCGGCGGAATTCATGGCTAG TATCAAACAAATAG-3′ containing the ATG start codon, introduced an *Eco*RI restriction site (underlined), and the carboxyl terminal primer 5′-GCGGCG TCTAGATCACTTGA TCCCCTGAGTCTTC-3′, including the stop codon, introduced an *Xba*I restriction site. PCR was carried out using *Taq* DNA polymerase (Promega, Madison, WI) at 94 °C for 2 min, 35 cycles of 94 °C for 45 s, 60 °C for 45 s, and 72 °C for 1.5 min; followed by a 10 min extension at 72 °C. The PCR fragment was gel purified using a Sephaglas Bandprep kit (New England Biolabs, Beverly, MA) and ligated into pGEM-T-easy vector (Promega). The pGEM-T-MtANR plasmid was transformed into *E. coli* DH5α competent cells for sequence analysis. The open reading frame was then excised by digestion with *Eco*RI and *Xba*I and re-ligated into *Eco*RI and *Xba*I digested pMAL-c2X vector as an N-terminal fusion to the maltose-binding protein (*MBP*) gene to generate the protein expression construct pMMtANR.

To clone AtANR for protein expression, total RNA from young siliques of *A. thaliana* cv Columbia was isolated using the Tri-Reagent kit (Molecular Research Center, Cincinnati, OH). First strand cDNA was synthesized from 4 μg total RNA from siliques by SuperscriptII reverse transcriptase (Invitrogen, Carlsbad, CA) according to the manufacturer's instructions. The *ANR* gene was amplified from 10 μl of the first strand cDNA by high fidelity Pfu DNA polymerase-mediated PCR using forward primer 5′-GGGCCCATGGAC CAGA CTCTTACACACACCGGA-3′ and reverse primer 5′-CCCAGATCTAGAATGAGACCAAAG ACTCATAT ACT-3′ at 94 °C for 5 min, 30 cycles of 94 °C for 1 min, 55 °C for 1 min, and 72 °C for 1.5 min, followed by a further 10 min extension at 72 °C. The PCR fragment was digested with *Nco*I and *Xba*I, and cloned into *Nco*I–*Xba*I digested pRTL2 to give the construct pSBP77, which was then sequenced. For expression of AtANR *in E. coli*, pSBP77 was digested with *Nco*I and then blunted with mung bean nuclease (New England BioLabs). The ANR coding region fragment was purified after digestion with *Xba*I, and ligated into

*Xmn*I and *Xba*I digested pMAL-c2X as an N-terminal fusion to the *MBP* gene to generate the protein expression construct pMAtANR.

pMMtANR, pMAtANR, and pMAL-c2X (as control vector) were transformed into NovaBlue (DE3) competent cells (Novagen, Madison, WI). A single colony harboring either construct or control vector was inoculated into 1 liter of LB broth containing 100 mg/liter ampicillin and cells were grown to an OD_{600} of 0.3 at 37 °C and 250 rpm. The cells were then transferred to 16 °C and grown to an OD_{600} of 0.6–0.7, at which point isopropyl-1-thio-β-D-galactopyranoside (IPTG) was added to a final concentration of 1 mM. The cells were harvested 24 h later by centrifugation at 3000 rpm at 4 °C for 15 min. Pellets were either used directly for enzyme extraction or stored at −80 °C.

Enzyme extraction and purification

All procedures were performed at 4 °C. Crude enzyme was extracted as described previously [12] and further purified on an amylose column. Three to 4 ml amylose homogenate (New England Biolabs) was loaded into a 2.5 × 16 cm column, and then washed and equilibrated with at least 10 volumes of washing buffer (20 mM Tris–HCl, pH 7.0, and 10 mM β-mercaptoethanol). The crude extract was diluted five times with washing buffer and then loaded onto the column at a flow rate of 1 ml/min. The column was washed with at least 15 column volumes of washing buffer and the MBP-ANR fusion protein eluted with washing buffer supplemented with 10 mM maltose. The fusion protein was concentrated to 1.5–10 μg/μl by passing through a 10,000 molecular weight cut-off Amicon Ultra (Millipore) membrane and then analyzed by electrophoresis on a 12% SDS–polyacrylamide gel stained with 0.25% Coomassie brilliant blue (R250). ANR protein was separated from MBP by protease cleavage with Factor Xa (New England Biolabs) following the manufacturer's protocol.

Enzyme assays and determination of kinetic parameters

All enzyme assays were performed by measuring appearance of flavan 3-ol products by HPLC after stopping reactions after the required time periods. For determination of temperature optimum, enzyme assays were carried out for 30 min in a total volume of 200 μl containing 100 mM Tris–HCl, pH 7.0, 100 μM cyanidin chloride, 2 mM NADPH, and 50–100 μg MBP-ANR or 30 μg purified cleaved ANR. Determination of pH dependence and reaction kinetics was performed with MBP-ANR fusion proteins.

pH profiles for MtANR and AtANR were determined at their respective temperature optima of 45 °C (MtANR) and 55 °C (AtANR) with 30 min incubations in a final volume of 200 μl consisting of 50 mM citrate/phosphate buffer, pH 4.0–7.0, 50 mM Mes buffer, pH 5.0–7.0 or 100 mM Tris–HCl buffer, pH 7.0–8.8, 100 μM cyanidin, 2 mM NADPH, and 50–100 μg purified fusion protein.

Kinetic constants for NADPH or NADH were determined at the respective temperature optima of MtANR and AtANR in a total volume of 200 μl containing 50 mM Mes buffer, pH 6.0 (for MtANR) or 100 mM Tris–HCl, pH 8.0 (for AtANR), 100 μM cyanidin, 0–12 mM NADPH or NADH, and 100 μg MBP-fusion protein, with 30 min incubation. Kinetic constants for anthocyanidin substrates were likewise determined in a total volume of 200 μl containing 100 μg MBP-fusion protein, 0–300 μM cyanidin chloride or delphinidin chloride, or 0–500 μM pelargonidin chloride, and 2 mM NADPH.

To determine the effects of flavonoids and Na^+ ions, enzyme assays were carried out at the respective temperature and pH optima in a total volume of 200 μl containing 100 μg MBP-fusion protein, 100 μM cyanidin chloride, 2 mM NADPH, and either (±)-DHQ (0–1 mM), (+)-catechin (0–1 mM), quercetin (0–0.1 mM) or NaCl (0–400 mM).

To determine whether MtANR or AtANR can epimerize or racemize the flavan-3-ol products, assays were carried out at the respective temperature and pH optima in a total volume of 200 μl containing 100 μg fusion protein, 2 mM NADPH, and 35–70 μM (−)-epicatechin or 50–100 μM (±)-catechin in the presence or absence of 100 μM cyanidin. Control experiments were performed under the same conditions with buffer or boiled enzyme instead of active enzyme.

All enzyme reactions were initiated by adding enzyme and stopped by adding 1 ml ethyl acetate with vigorous vortexing for 1 min, and then centrifuged for 1 min at 10,000 rpm. The ethyl acetate supernatant phase (0.9 ml) was transferred to a new 1.5 ml microcentrifuge tube and dried under nitrogen gas at room temperature. Residues were dissolved in 50 μl HPLC grade methanol for HPLC analysis.

HPLC analysis and data integration

HPLC analysis used a HP 1100 machine and C18 reversed phase column with UV detection at 280 nm for (−)-epicatechin, (±)-catechin, (+)-catechin, (−)-epiafzelechin, and (−)-afzelechin, and at 270 nm for (−)-gallocatechin and (−)-epigallocatechin. The solvent system consisted of water (solvent A) and acetonitrile (solvent B). The gradient program consisted of ratios of solvent A to solvent B of 95:5 (0–5 min), 95:5 to 93:7 (5–7 min), 93:7 (7–25 min), 93:7 to 60:40 (25–40 min), 60:40 to 5:95 (40–40.5 min), and 5:95 (40.5–49.5 min). Forty μl samples was injected with a flow rate of 1.5 ml per min. Product peaks were identified by retention time and UV spectrum as previously described [12]. Authentic

standards of (±)-catechin, (−)-epicatechin, (−)-gallocatechin, and (−)-epigallocatechin were injected for reference.

Each experiment was performed in triplicate and repeated at least once. Product formation was estimated by integrating peak area using HP Chemstation Software. Amounts of reaction products were calculated based on established standard curves using authentic samples. Due to lack of available standards of (−)-epiafzelechin and (−)-afzelechin, the products produced from pelargonidin were simply estimated by integrating peak areas. Values could not be calculated with pelargonidin as substrate. The enzymatic products consisted of two isomers. Initial reaction velocity was calculated as the total sum of the products, i.e., (−)-catechin and (−)-epicatechin, (−)-afzelechin and (−)-epiafzelechin, or (−)-gallocatechin and (−)-epigallocatechin. K_m, V_{max}, $[S]_{0.5}$, and n_H values were calculated through various plots of initial reaction velocity versus substrate concentration. V_{max} values were not calculated for pelargonidin due to lack of authentic standards of (epi)-afzelechin for absolute quantitation.

Results

Sequence comparison of MtANR and AtANR

MtANR and AtANR (from *A. thaliana* ecotype Columbia) share only 60% amino acid sequence identity. MtANR consists of 338 amino acids with a molecular weight (MW) of 36,977 Da, whereas AtANR consists of 340 amino acids, with an MW of 37,904 Da.

Both MtANR and AtANR contain the classical Rossmann dinucleotide-binding domain [24] characterized by a conserved glycine rich amino acid sequence fingerprint of either GXGXXA (such as found in monodehydroascorbate reductases, MDAR) [25] or GXXGXXG (such as found in plant dihydroflavonol reductases, DFR) (Fig. 2). Within the GXXGXXG consensus, MtANR has the F22 conserved in DFR homologs but AtANR has N at this position (Fig. 2).

Expression and purification of ANR-MBP fusion protein

The MtANR and AtANR open reading frames were amplified by PCR and cloned into the protein expression vector pMAL-c2X immediately downstream of the MBP to facilitate protein purification. MBP fusion proteins have often been used for studying enzyme kinetics, three-dimensional structures, and catalytic mechanisms [25–27]. The constructs were transformed into *E. coli* NovaBlue (DE3). MtANR and AtANR MBP fusion proteins localized to inclusion bodies when expressed in *E. coli* at 37 °C, but were recovered as soluble enzymes following expression at 16 °C. This expression system allowed for the production of from 10 to 20 mg ANR protein per liter of culture, suitable amounts for crystallization studies. Fusion proteins were purified by amylose affinity chromatography resulting in a single major band of approximatly 70 kDa by denaturing SDS–PAGE (Fig. 3A).

To ensure that the presence of the MBP did not adversely affect the properties of ANR, we compared the specific activities and temperature optima of purified recombinant MBP-MtANR and cleaved "native" MtANR; the temperature optima were identical (45 °C), and the specific activity of the native protein was reduced by 30% compared to that of the MBP fusion. Significant protein losses occurred during separation of ANR from MBP following cleavage with Factor Xa at 4 °C, although there is no Factor Xa cleavage site in the ANR protein, and this may explain the small reduction in specific activity.

Effects of temperature, pH, and NaCl on ANR activities

The ANR reaction was linear over the 30 min time period used for standard assays. The temperature optima (reflecting the composite of reaction rate and protein

cDNA gene bank accession#	Enzyme		Sequence (with position #)	Species
AT1G61720	ANR	12	K A C V I G G T G N L A S I L I K H L L	At-col
AAF23859.1	ANR	12	K A C V I G G T G N L A S I L I K H L L	At-ws
AAN77735.1	ANR	13	K A C V I G G T G F V A S L L I K Q L L	Mt
JQ1688	DFR	7	T V C V T G A S G F I G S W L V M R L L	At-col
AY389346	MtDFR1	7	T V C V T G A S G F I G S W L V M R L M	Mt
AY389347	MtDFR2	7	T V C V T G A S G F I G S W L V M R L M	Mt
Amino acid fingerprint			G X X G X X G/A	
Consensus			* * * * * * * *	

Fig. 2. Clustal X alignment showing the high amino acid sequence conservation between dihydroflavonol reductases (DFR) and ANRs at the 5′ amino terminal regions including the Rossmann dinucleotide (NADPH/NADH)-binding domain. At-col, *A. thaliana* ecotype Columbia; At-ws, *A. thaliana* ecotype Ws (Wassilewskijia); Mt, *M. truncatula*; and MtDFR1 and 2, *M. truncatula* dihydroflavonol reductase orthologs 1 and 2 (GenBank Accession Nos. AY389346 and AY389347).

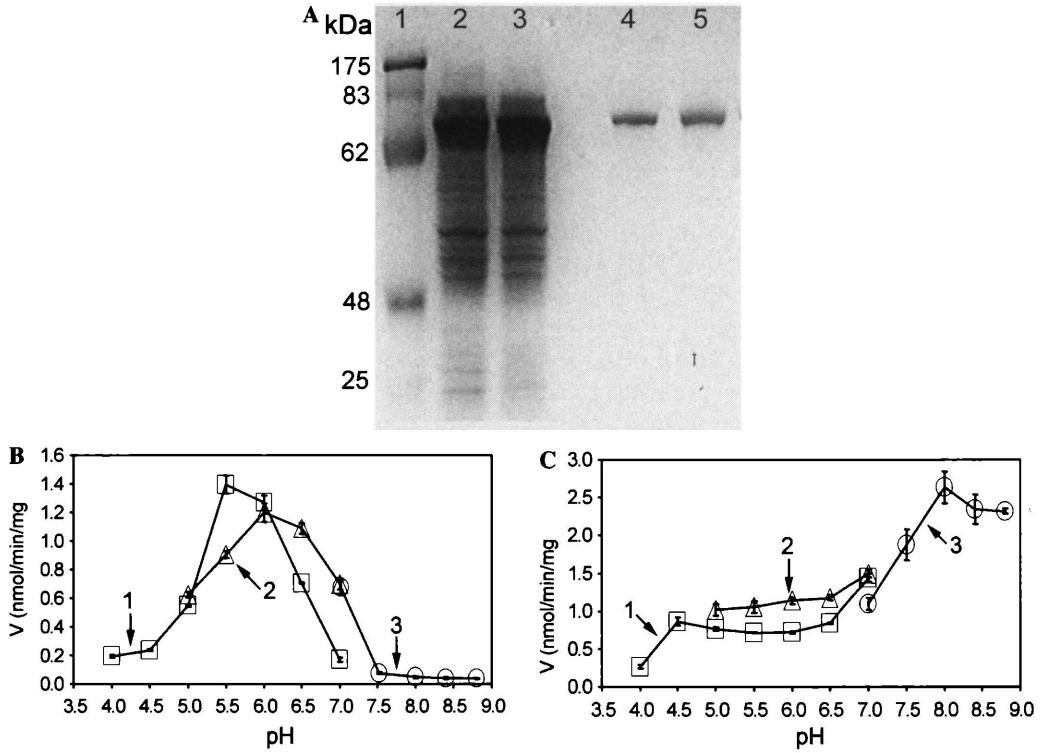

Fig. 3. ANR fusion protein expression in *E. coli* and determination of pH optima. (A) SDS–polyacrylamide (12%) gel electrophoresis of *E. coli*-expressed MBP-MtANR and MBP-AtANR fusion proteins stained with Commassie brilliant blue G250. Lane 1, prestained protein mass markers (New England Biolabs); lane 2, 20 μg crude extract from *E. coli* harboring pMMtANR; lane 3, 20 μg crude extract from *E. coli* harboring pMAtANR; lane 4, 2 μg purified MBP-MtBAN; and lane 5, 2 μg purified MBP-AtBAN. (B) The effect of pH on MtANR activity. (C) The effect of pH on AtANR activity. In (B) and (C), curve 1 is for 50 mM citrate-phosphate, curve 2 for 50 mM Mes, and curve 3 for 100 mM Tris–HCl.

stability) of both MBP-MtANR and MBP-AtANR reactions in vitro were quite similar (Table 1). However, dramatic differences were observed in pH dependence, with MtANR having a weakly acidic pH optimum and AtANR showing maximum activity at weakly basic pH (Figs. 3B and C). The pH optimum of MtANR was 5.5 in 50 mM citrate/phosphate but 6.0 in 50 mM Mes buffer (Fig. 3B). Addition of increasing concentrations of Na^+ to 50 mM Mes buffer (pH 6.0) indicated that MtANR activity is inhibited by Na^+ concentrations above 200 mM. This may explain the discrepancy between pH optima in citrate/phosphate and Mes buffer. NaCl concentrations up to 400 mM did not inhibit AtANR.

Co-enzyme requirements of MtANR and AtANR

Significant differences between MtANR and AtANR were observed in their co-enzyme requirements. MtANR used either NADPH or NADH as co-substrates (Figs. 4A and B). Double reciprocal plots of $1/V$

Table 1
Kinetic properties of MtANR and AtANR

	MtANR				AtANR			
	V_{max} (nmol/min mg)	K_m (μM)	k_{cat} (min^{-1})	k_{cat}/K_m ($M^{-1}s^{-1}$)	V_{max} (nmol/min mg)	K_m (μM)	k_{cat} (min^{-1})	k_{cat}/K_m ($M^{-1}s^{-1}$)
Substrates								
Cyanidin	1.2 ± 0.7	12.9 ± 0.4	10.8	1.4×10^4	10.0 ± 1.8	73.9 ± 5.9	62.7	1.4×10^4
Pelargonidin		14.5				52.8 ± 3.9		
Delphinidin	60.6	49.8 ± 10.8	80.3	2.7×10^4	0.9 ± 0.02	17.8 ± 1.5	3.5	0.3×10^4
Cofactors								
NADPH	0.4 ± 0.01	450 ± 120			$n_H = 3.3 \pm 0.3$, $[S]_{0.5} = 125.5 \pm 0.7$ μM			
NADH	0.3 ± 0.1	940 ± 155			NR*			
Temperature:		45 °C			55 °C			

*NR, no reaction.

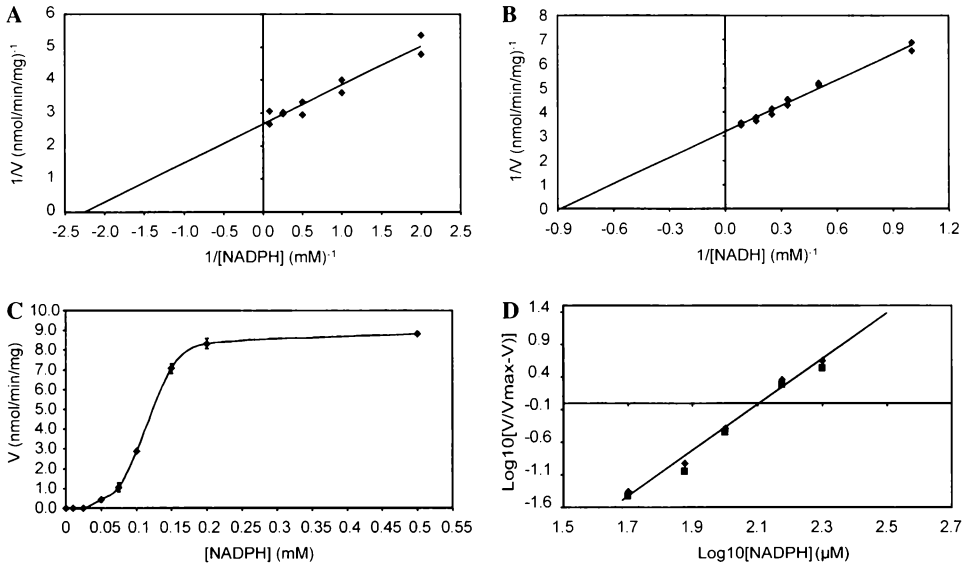

Fig. 4. Kinetics of MtANR (A,B) and AtANR (C,D) with NADPH and/or NADH. The initial velocity was recorded as the rate of production of (−)-epicatechin plus (−)-catechin from the substrate cyanidin (100 μM) at varying NAD(P)H concentrations. (A) Double reciprocal plot for MtANR with NADPH. (B) Double reciprocal plot for MtANR with NADH. (C) Plot of initial velocity versus [NADPH] for AtANR. (D) Hill plot of $\log[V/(V_{max} - V)]$ versus log [NADPH] for AtANR with NADPH.

versus 1/[NADPH] or 1/[NADH] for MtANR indicated classic Michaelis–Menten steady-state kinetics (Figs. 4A and B), with a lower K_m and higher V_{max}/K_m for NADPH than for NADH (Table 1). In contrast, AtANR did not use NADH as co-substrate and the saturation curve for NADPH was sigmoid rather than hyperbolic, suggesting positive cooperativity (Fig. 4C). A plot of log $(V/V_{max} - V)$ versus log [NADPH] was a straight line (Fig. 4D), from which a Hill co-efficient (n_H) of 3.3 and $[S]_{0.5}$ of 125 μM were calculated (Table 1).

Properties of MtANR and AtANR towards anthocyanidin substrates

MtANR and AtANR showed significant difference in their steady-state kinetics with anthocyanidin substrates. At optimum pH, temperature, and NADPH concentration, MtANR exhibited Michaelis–Menten kinetics with cyanidin, pelargonidin, and delphinidin (Figs. 5A–C). The double reciprocal plots indicated the highest K_m for delphinidin, followed by pelargonidin and then cyanidin (Table 1). However, MtANR had its highest V_{max} value for delphinidin (Table 1), resulting in a twofold higher k_{cat}/K_m ratio for delphinidin compared to cyanidin.

AtANR differed markedly from MtANR in its kinetic properties towards cyanidin and pelargonidin (Figs. 5E–H), with the reaction velocity decreasing with anthocyanidin concentrations above 100–150 μM (Figs. 5E and G). At lower substrate concentrations, the reaction followed classic Michaelis–Menten kinetics (Figs. 5E and G). The upturn in the plots of $1/V$ versus 1/[cyanidin] or 1/[pelargonidin] on approaching the $1/V$ axis (Figs. 5F and H) is indicative of substrate inhibition. This could result from low levels of a non-competitive inhibitor (perhaps a specific ionization product of the anthocyanidin, as depicted in Fig. 1B) present in the substrate sample. The kinetics towards cyanidin and pelargonidin were therefore fitted to the following velocity equation for a substrate plus non-competitive inhibitor:

$$v/V_{max} = [S]/\{K_m + [S](1 + xK_m/K_i + x[S]/K_i)\},$$

where K_m is the substrate concentration at $1/2V_{max}$, x represents a coefficient for [I] where $[I] = x[S]$ in the substrate solution, and K_i is the inhibitor constant defined as $\{[E][I]\}/[EI]$. This analysis facilitated calculation of apparent K_m values for cyanidin and pelargonidin as well as a V_{max} for cyanidin (Table 1).

In contrast to the above observations with cyanidin and pelargonidin, AtANR displayed classical Michaelis–Menten kinetics towards delphinidin (Fig. 5D). The K_m of AtANR was highest for cyanidin, followed by pelargonidin and then delphinidin (Table 1). Nevertheless, the k_{cat}/K_m ratio was highest with cyanidin, suggesting that this may be the preferred substrate in vivo.

Inhibitors of MtANR and AtANR

The purity of the commercial cyanidin and pelargonidin substrates was checked by HPLC and was 97–99%. Minor contamination by flavonols (kaempferol and quercetin) and dihydroflavonols (dihydroquercetin) was observed. (±)-DHQ, quercetin, and (+)-catechin (2R, 3S-2, 3-*trans*-flavan-3-ol) (Fig. 6A) were tested for their effects on ANR activity in vitro. (+)-Catechin did

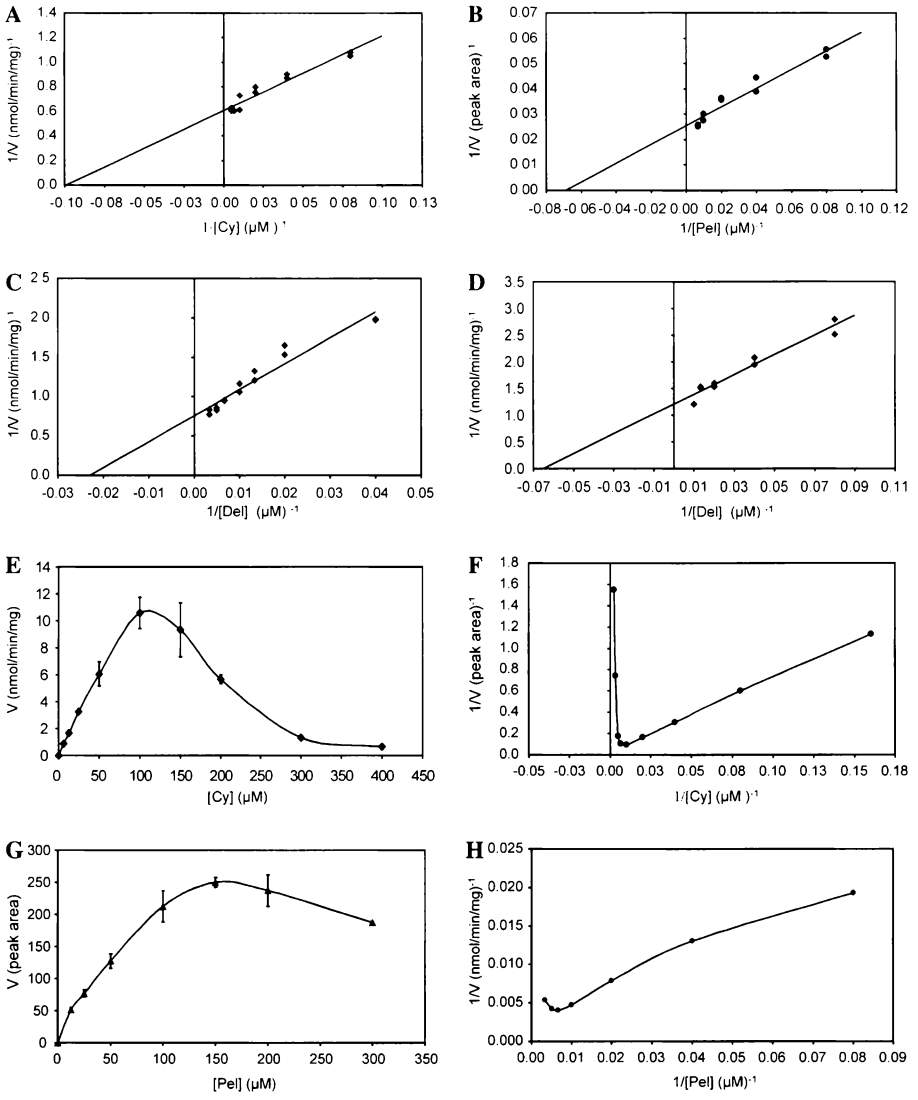

Fig. 5. Kinetics of MtANR and AtANR with cyanidin, pelargonidin, and delphinidin. The initial velocity was recorded as the rate of production of (−)-epicatechin plus (−)-catechin from varying concentrations of cyanidin (Cy), or the sums of the corresponding products from pelargonidin (Pel) or delphinidin (Del), respectively, at a NADPH concentration of 2 mM. (A) Double reciprocal plot for MtANR with cyanidin. (B) Double reciprocal plot for MtANR with pelargonidin. (C) Double reciprocal plot for MtANR with delphinidin. (D) Double reciprocal plot for AtANR with delphinidin. (E) Plot of initial velocity versus [cyanidin] for AtANR. (F) Double reciprocal plot for AtANR with cyanidin. (G) Plot of initial velocity versus [pelargonidin] for AtANR. (H) Double reciprocal plot for AtANR with pelargonidin.

not inhibit MtANR activity (Fig. 6B), but inhibited AtANR by 50% at 0.5 mM (Fig. 6C). (±)-DHQ did not inhibit MtANR (Fig. 6D), but inhibited AtANR at concentrations as low as 25 μM (Fig. 6E). Quercetin strongly inhibited both MtANR and AtANR (Figs. 6F and G).

The origin of the epimerization products of the ANR reaction

We have previously shown that ANR converts cyanidin into (−)-epicatechin as the major product, with (−)-catechin as a minor product [12]. Likewise, (−)-epiafzelechin is the major product and (−)-afzelechin the minor product from pelargonidin. Equal amounts of (−)-gallocatechin and (−)-epigallocatechin are formed from delphinidin [12]. The question therefore arises as to whether (−)-catechin, (−)-afzelechin, and (−)-gallocatechin are formed by non-enzymatic epimerization at C_2 of the major products (−)-epicatechin, (−)-epiafzelechin, and (−)-epigallocatechin, respectively, or whether they are separate reaction products formed by the enzyme itself. To address this question, MtANR or AtANR was incubated with (−)-epicatechin or (±)-catechin in the presence of NADPH, and parallel controls were included in which active enzyme was replaced with boiled enzyme or buffer. No epimerization or racemization of (−)-epicatechin or (−)-catechin into the corresponding

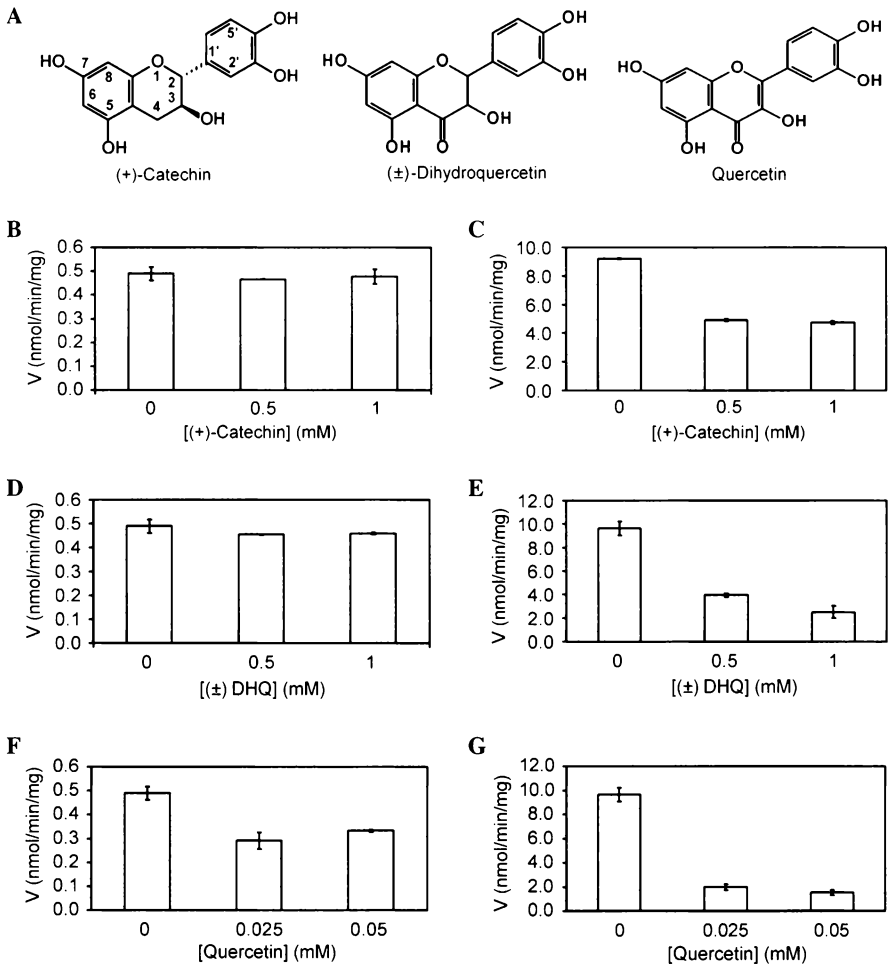

Fig. 6. Effects of flavonoids on ANR activity. Initial velocities were recorded for production of (−)-epicatechin and (−)-catechin from cyanidin. (A) Chemical structures of (+)-catechin, (±)-dihydroquercetin (DHQ), and quercetin. (B,C) The effect of (+)-catechin on MtANR (B) and AtANR (C). (D,E) The effect of (±)-dihydroquercetin on MtANR (D) and AtANR (E). (F,G) The effect of quercetin on MtANR (F) and AtANR (G).

(−)-catechin or (−)-epicatechin, respectively, was observed under any of these conditions if Mes buffer was used. However, incubation of (−)-epicatechin in 100 mM Tris–HCl, pH 7, at temperatures above 30 °C even without enzyme resulted in epimerization to catechin, suggesting that the (−)-catechin observed as a minor product in the enzyme assays might result from chemical epimerization rather than an ability of ANR to produce both 2R, 3R-2, 3-*cis*-and 2S, 3R-2, 3-*trans*-flavan-3-ol isomers.

Discussion

Amino acid sequence comparison and biochemical differences between MtANR and AtANR

MtANR and AtANR share only 60% amino acid sequence identity. Both enzymes contain the conserved Rossmann dinucleotide-binding domain at their amino-termini [24,28,29]. To date, there are few available *ANR* gene sequences from different plant species, and, to the best of our knowledge, no other reports of ANR substrate/co-substrate specificity. However, it seems likely that the two amino acid differences between the dinucleotide-binding domains of MtANR and AtANR (F22 and V23 in MtANR corresponding to N21 and L22 in AtANR) may be related to the different specificities of the two enzymes for NADPH and NADH. Examples exist where only a single amino acid change can alter co-factor binding specificity. For example, rat NADPH-dependent cytochrome P-450 reductase cannot use NADH as cofactor, but mutation of Trp 677 to Ala generates an enzyme with quite good NADH turnover [30]. Detailed structural studies of MtANR and AtANR will be necessary to definitively explain their different co-factor specificities.

The kinetics of MtANR for NADPH followed the usual Michaelis–Menten behavior observed with many reductases, whereas those for AtANR were sigmoidal and indicative of positive cooperativity, with NADPH acting as co-substrate and modulator. Other reductases,

such as ribonucleotide reductase [31], also show allosteric behavior, and very different kinetics of enzymes with NADPH do not necessarily require extensive differences in amino acid sequence [32,33]. The non-linear kinetics of AtBAN could reflect the operation of the two successive hydride transfers in the overall ANR reaction.

The turnover (k_{cat}) of both MtANR and AtANR was quite slow. Both enzymes reduce cyanidin, pelargonidin, and delphinidin, indicating that the B-ring hydroxylation pattern is not critical for catalysis. However, the relative binding affinities for the three substrates differ, with MtBAN exhibiting decreasing K_m values in the order delphinidin > pelargonidin > cyanidin, and AtBAN exhibiting the inverse relationship. Nevertheless, both enzymes had the same k_{cat}/K_m ratio for cyanidin, which may be the major in vivo substrate for both enzymes, consistent with the presence of (−)-epicatechin residues as the major building blocks in the CTs of both *A. thaliana* and *M. truncatula*. Similar to ANR, different dihydroflavonol reductases (DFR) from *M. truncatula*, *Malus domestica*, and *Pyrus communis* showed significantly different kinetics towards DHQ and dihydrokaempferol, which differ in B-ring hydroxylation pattern [34,35].

High cyanidin or pelargonidin concentrations inhibit AtANR but not MtANR. This inhibition may result from the presence of non-competitive inhibitor(s) in the substrate preparations. Quercetin inhibited both MtANR and AtANR activities, whereas (+)-catechin and (±)-DHQ inhibited AtANR but not MtANR. *M. truncatula* produces (+)-catechin as a component of the seed coat CT, whereas the *Arabidopsis* CT does not contain (+)-catechin [15]. (−)-Epicatechin did not inhibit MtANR or AtANR over the tested concentration range. In the absence of information on the pool sizes of dihydroflavonols and flavan 3-ols in the seed coat endothelium, it is not possible to conclude whether the above inhibitory effects are of physiological significance.

Reaction mechanisms for reduction of anthocyanidins to flavan-3-ols

The discovery of ANR explains the inversion of stereochemistry at C_3 during the biosynthesis of (−)-epicatechin from leucoanthocyanidin. The heterocyclic C-ring of anthocyanidins, formed from chiral leucoanthocyanidins, has two double bonds, at O_1–C_2 and C_3–C_4, and is therefore achiral. ANR reduces anthocyanidins to flavan-3-ols through NADPH-mediated reduction at C_2 and C_3, allowing for the inversion of stereochemistry at C_3. The (−)-catechin (minor product) observed in enzymatic reactions may be produced by non-enzymatic epimerization at C_2 of (−)-epicatechin under the reaction conditions used. (−)-Catechin has recently been shown to exert strong alleopathic effects and to be a major factor for colonization by the destructive non-indigenous spotted knapweed in North America [36]. Analysis of the properties of ANR from this weedy species may reveal alternative routes for the biosynthesis of (−)-catechin.

Although anthocyanidins are often depicted as having a positive charge associated with the oxygen of the heterocyclic ring, it is recognized that the charge may be delocalized [19–21]. Assessment of charge distributions on the flavylium cation through molecular orbital calculations suggests that electrophilic attack can occur at positions C_8, C_6 and various B-ring sites, and nucleophilic attack principally at C_2 and C_4 [16,19–21,37,38]. This is consistent with the facile in vitro chemical synthesis of flavan-3-ols through reduction of anthocyanidins with PtO_2 in a hydrogen atmosphere [38]. Complete hydrogenation of cyanidin or its pentamethyl ether, and fisetinidin and butinidin, resulted in the corresponding reduced products (±)-epicatechin and its pentamethyl ether, (±)-2,3-*cis*-3,3′,4′,7′-tetrahydroxyflavan, and (±)-2,3-*cis*-3′,4′,7-trihydroxyflavan, respectively [38]. Hrazdina also synthesized (±)-3′-*O*-methylepicatechin, (±)-3′,5′-di-*O*-methylepigallocatechin and (±)-3′-*O*-methylepigallocatechin from peonidin (3′-*O*-methylcyanidin), malvidin (3′,5′-di-*O*-methyldelphinidin), and petunidin (3′-*O*-methyldelphinidin), respectively, with sodium borohydride in ethanol or methanol [38]. The intermediates of the in vitro reduction were the flav-3-en-3-ols and flav-2-en-3-ols (Fig. 7), which are stable on exposure to air and in aqueous acidic solution. The initial reduced flavenes are in equilibrium with the corresponding 3-keto form (flavan-3-one tautomer) (Fig. 7), which are then further reduced to the corresponding flavan-3-ols [39,40].

Based on the above considerations, it is possible to postulate four possible enzymatic reduction sequences for the ANR reaction (Fig. 7). In mechanism **I-a**, the first hydride ion provided by NADPH/NADH nucleophilically attacks C_2 to form a stable flav-3-en-3-ol, the configuration of the C_2-aryl group being 2R with hydride addition by way of the β-face (addition to the α-face would be necessary to account for enzymatic production of the 2S configuration of the minor product (−)-catechin). NADPH/NADH then provides a second hydride ion to attack C_4, and a proton from the medium then quenches the charge at C_3, thereby reducing the C_3–C_4 double bond. The configuration of the C_3-hydroxyl group as 3R or 3S is also dependent upon the direction of hydride ion addition. This will again be from the β-face to result in the formation of 2R, 3R-2, 3-*cis*-flavan-3-ols.

In mechanism **I-b**, the first step is the same as in **I-a**. In the second step, ANR transforms the flav-3-en-3-ol intermediate into its tautomeric flavan-3-one (Fig. 7) followed by reduction by NADPH/NADH at C_3 and

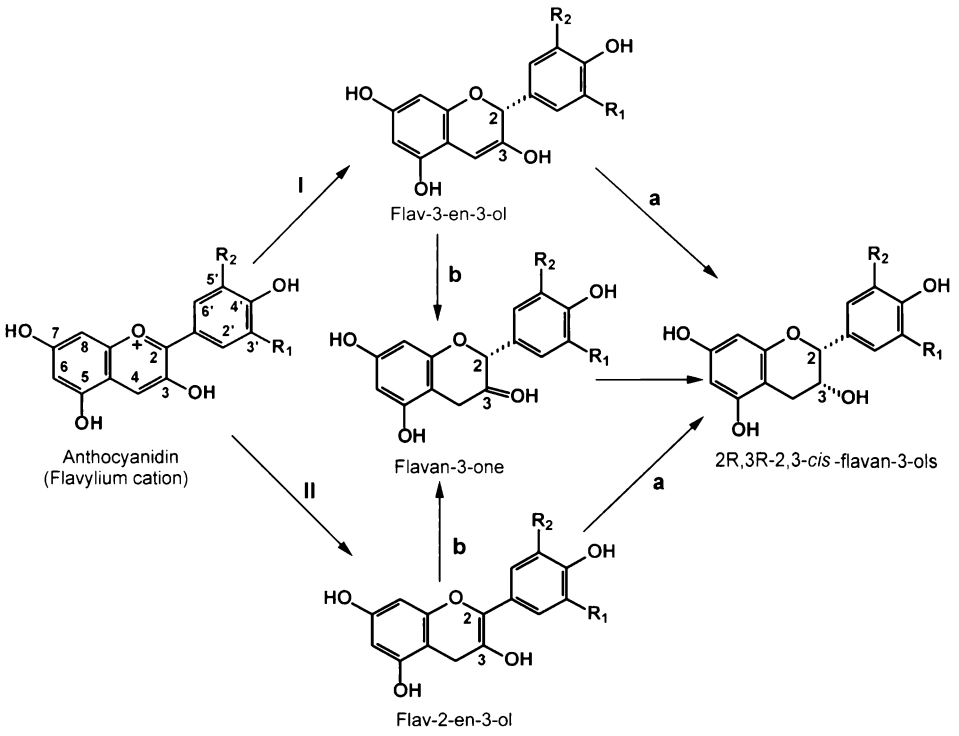

Fig. 7. Possible reaction sequences for conversion of anthocyanidins into 2,3-*cis*-flavan-3-ols by ANR. Alternative stereochemistries at C2 and C3 are theoretically possible through routes IIa and IIb, and at C3 through routes Ia and Ib. R_1, R_2 = H or OH.

acquisition of a proton from the medium at the 3-keto oxygen to complete the conversion to flavan-3-ols. The 3R configuration of the C_3-hydroxyl group would result from hydride attack from the β-face. This reaction sequence is supported by in vitro conversion of flavan-3-one into (+)-catechin and (−)-epicatechin [40]. Formation of 2R, 3S-(+)-catechin, the starter molecule for many CTs [40], could theoretically occur through an ANR reaction with hydride attack at C_3 from the α-face. However, although ANR might produce the two different stereoisomers at C_2, only the 3R epimer is produced at C_3 [12]. A completely different pathway, proceeding through a leucoanthocyanidin reductase (LAR), has been proposed to account for production of (+)-catechin [40]. This pathway has received support from the recent cloning of a LAR from *D. uncinatum* (17), although the stereochemistry of the product was not directly determined.

In the second group of mechanisms, the first step is nucleophilic attack of a hydride ion at C_4 to give an achiral flav-2-en-3-ol. In mechanism **II-a**, the C_2–C_3 double bond is then reduced by NADPH/NADH to produce the final flavan-3-ol, in which the configurations of the C_2-aryl and C_3-hydroxyl groups are again dependent on the directions of hydride addition. In mechanism **II-b**, the flav-2-en-3-ol is reduced at C_2 to form the tautomeric flavan-3-one, with the configuration of the C_2-aryl group associated with the direction of hydride addition from the α- or β-face; the 3-keto group is then reduced to produce the flavan-3-ol, with introduction of stereochemistry at C_3.

The proposed group **II** reaction mechanisms might explain why quercetin is a strong inhibitor of MtANR and AtANR. The structure of quercetin is similar to that of 2-flaven-3-ols, and the enzyme may be able to bind quercetin resulting in loss of ability to convert flav-2-en-3-ol intermediates to flavan-3-ols.

Other possibilities for the ANR reaction mechanism cannot be excluded, in particular the possibility that the initial substrate is not the flavylium ion but the anhydro or quinoidal base that will exist in solution at the pH optima of MtBAN and AtBAN. The pseudobase can also exist at pH 5, close to the pH optimum of MtANR (pH 6.0) but not AtANR (pH 8.0). Trapping and isolation of intermediates from the ANR enzymatic reaction, particularly following reaction in the presence of stereospecifically labeled ^{3}H-NADPH, together with analysis of the three-dimensional structures of different ANR enzymes, will eventually allow assignment of reaction mechanism(s) to this new class of plant natural product reductase.

Acknowledgments

This work was supported by the Samuel Roberts Noble Foundation and Forage Genetics International. We thank Drs. Daneel Ferreira (University of

Mississippi) and Lahoucine Achnine (Noble Foundation) for critical reading of the manuscript, and Dr. Ferreira for useful discussions on the potential reaction mechanisms of ANR and the chemistry of catechins.

References

[1] L.R. McMahon, T.A. McAllister, B.P. Berg, W. Majak, S.N. Acharya, J.D. Popp, B.E. Coulman, Y. Wang, K.J. Cheng, Can. J. Plant. Sci. 80 (2000) 469–485.
[2] D.J. Peters, C.P. Constabel, Plant J. 32 (2002) 701–712.
[3] R.A. Dixon, L.W. Sumner, Plant Physiol. 131 (2003) 878–885.
[4] D. Bagchi, M. Bagchi, S.J. Stohs, D.K. Das, S.D. Ray, C.A. Kuszynski, S.S. Joshi, H.G. Pruess, Toxicology 148 (2000) 187–197.
[5] A. Scalbert, S. Deprez, I. Mila, A.M. Albrecht, J.F. Huneau, S. Rabot, Biofactors 13 (2000) 115–120.
[6] H. Chen, A.L. Tappel, Free Radic. Biol. Med. 18 (1995) 949–953.
[7] M.T. Walters, A.P. Heasman, P.S. Hughes, J. Am. Soc. Brew. Chem. 55 (1997) 83–89.
[8] H. Hibasami, T. Komiya, Y. Achiwa, K. Ohnishi, T. Kojima, K. Nakanishi, K. Akashi, Y. Hara, Oncol. Rep. 5 (1998) 527–529.
[9] M. Serafini, R. Bugianesi, G. Maiani, S. Valtuena, S. De Santis, A. Crozier, Nature 424 (2003) 1013.
[10] K. Springob, J.-I. Nakajima, M. Yamazaki, K. Saito, Nat. Prod. Rep. 20 (2003) 288–303.
[11] T.A. Holton, E.C. Cornish, Plant Cell 7 (1995) 1071–1083.
[12] D.-Y. Xie, B.S. Sharma, N.L. Paiva, D. Ferreira, R.A. Dixon, Science 299 (2003) 396–399.
[13] S. Albert, M. Delseny, M. Devic, Plant J. 11 (1997) 289–299.
[14] M. Devic, J. Guilleminot, I. Debeaujon, N. Bechtold, E. Bensaude, M. Koornneef, G. Pelletier, M. Delseny, Plant J. 19 (1999) 387–398.
[15] S. Abrahams, G.J. Tanner, P.J. Larkin, A.R. Ashton, Plant Physiol. 130 (2002) 561–575.
[16] M.R. Koupai-Abyazani, J. McCallum, A.D. Muir, G.L. Lees, B.A. Bohm, G.H.N. Towers, M.Y. Gruber, J. Agric. Food Chem. 41 (1993) 565–569.
[17] G.J. Tanner, T.K. Francki, S. Abrahams, J.M. Watson, P.J. Larkin, A.R. Ashton, J. Biol. Chem. 278 (2003) 31647–31656.
[18] C.F. Timberlake, P. Bridle, in: J.B. Harborne, T.J. Mabry, H. Mabry (Eds.), The Flavonoids, Academic Press, New York, 1975, pp. 214–266.
[19] G. Bendz, A. Haglund, Acta Chem. Scand. 21 (1967) 2286–2287.
[20] G. Bendz, A. Haglund, Acta Chem. Scand. 21 (1967) 2287–2288.
[21] G. Bendz, A. Haglund, Acta Chem. Scand. 21 (1967) 2569.
[22] C.F. Timberlake, P. Bridle, Nature 212 (1966) 158–159.
[23] R. Brouillard, in: J.B. Harborne (Ed.), The Flavonoids: Advances in Research Since 1980, Chapman and Hall, London, 1988, pp. 525–538.
[24] C.A. Bottoms, P.E. Smith, J.J. Tanner, Protein Sci. 11 (2002) 2125–2137.
[25] M.S. Subramanian, A.B. Zilinskas, J. Biol. Chem. 269 (1994) 31129–31133.
[26] Y. Liu, A. Manna, R. Li, E.W. Martin, C.R. Murphy, L.A. Cheung, G. Zhang, Proc. Natl. Acad. Sci. USA 98 (2001) 6877–6882.
[27] J. Nakajima, Y. Tanaka, M. Yamazaki, K. Saito, J. Biol. Chem. 276 (2001) 25797–25803.
[28] R.K. Wierenga, M.C.H. De Maeyer, W.G.J. Hol, Biochemistry 24 (1985) 1346–1357.
[29] E.C. Lee Elmore, T.D. Porter, J. Biol. Chem. 277 (2002) 48960–48964.
[30] S.P. Hendricks, C.K. Mathews, J. Biol. Chem. 273 (1998) 29512–29518.
[31] B. Santamaría, A.M. Estévez, O.H. Martínez-Costa, J.J. Aragón, J. Biol. Chem. 277 (2002) 1210–1216.
[32] Y. Ikeda, T. Tanaka, T. Noguchi, J. Biol. Chem. 272 (1997) 20495–20501.
[33] T.C. Fischer, H. Halbwirth, B. Meisel, K. Stich, G. Forkmann, Arch. Biochem. Biophys. 412 (2003) 223–230.
[34] D.-Y. Xie, L.A. Jackson, J.D. Cooper, D. Ferreira, N.L. Paiva, Plant Physiol. (2003) in press.
[35] H.P. Bais, R. Vepachedu, S. Gilroy, R.M. Callaway, J.M. Vivanco, Science 301 (2003) 1377–1380.
[36] W.E. Kurtin, P.-S. Song, Tetrahedron 24 (1968) 2255–2267.
[37] E. Nilsson, Ark. Kemi 31 (1969) 111–119.
[38] G. Hrazdina, Phytochemistry 11 (1972) 3491–3496.
[39] J. Coetzee, E. Malan, D. Ferreira, Tetrahedron 56 (2000) 1819–1824.
[40] H.A. Stafford, in: H.A. Stafford (Ed.), Flavonoid Metabolism, CRC Press, Boca Raton, 1990, pp. 63–99.